Phenotype-specific expression of T-type calcium channels in neurons of the major pelvic ganglion of the adult male rat

Yu Zhu, Elizabeth L. Zboran and Stephen R. Ikeda*

Department of Pharmacology and Toxicology, Medical College of Georgia, Augusta, GA 30912-2300, USA

1. Neurons from the major pelvic ganglia (MPG) of adult male rats were enzymatically dissociated and the neurochemical phenotype and Ca^{2+} current properties examined.

2. Neurons were divided into two subpopulations based on the presence or absence of low threshold T-type Ca^{2+} channels. The subpopulation of neurons expressing T-type Ca^{2+} channels was characterized by a mean diameter of 34 μm, a mean membrane capacitance (C_m) of 72 pF, tyrosine hydroxylase immunoreactivity (TH-IR), a lack of NADPH diaphorase (NADPHd) reactivity and a high degree of α_2-adrenoceptor-mediated Ca^{2+} current inhibition (60%).

3. The subpopulation of neurons without overt T-type Ca^{2+} channels had a mean diameter of 23 μm, a mean C_m of 30 pF, a lack of TH-IR and a moderate degree of α_2-adrenoceptor-mediated Ca^{2+} current inhibition (27%). About 50% of this subpopulation stained positively for NADPHd.

4. The contribution of high threshold N-type Ca^{2+} channels (60–70%), as determined from ω-conotoxin GVIA inhibition, and L-type Ca^{2+} channels (< 10%), as determined from nifedipine inhibition, to the whole-cell Ca^{2+} current was similar for both subpopulations of neurons.

5. These data indicate that the MPG contain at least two subpopulations of postganglionic neurons, i.e. adrenergic and non-adrenergic, with distinct electrophysiological and neurochemical properties. Furthermore, we propose that the presence or absence of T-type Ca^{2+} channels provides an electrophysiological means of identifying adrenergic and non-adrenergic phenotype, respectively, in neurons of the male rat MPG.

Neurons of the rat major pelvic ganglia (MPG) provide innervation to the pelvic viscera and external genitalia (Langworthy, 1965; Dail, Evan & Eason, 1975). Anatomically, the MPG are unique amongst autonomic ganglia in that a mixture of both sympathetic and parasympathetic postganglionic neurons reside within the same ganglion capsule (Dail, 1992). Functionally, neurons of the MPG of male rats are involved in physiologically complex processes such as micturation (de Groat, Booth & Yoshimura, 1992) and penile erection (de Groat & Booth, 1992). During pathological processes involving these functions, alterations in MPG neuron structure and function have been observed. For example, bladder outlet obstruction produces a marked hypertrophy of MPG neurons innervating the bladder (de Groat *et al.* 1992), and decreased testosterone levels have been documented to produce erectile dysfunction (Mills, Wiedmeier & Stopper, 1992), possibly resulting from functional alterations in MPG neurons (Giuliano, Rampin, Schirar, Jardin & Rousseau, 1993). Thus, the rat MPG provides a useful model system for studying the autonomic control of pelvic organs during normal and pathological conditions.

Since it is established that Ca^{2+} entry via voltage-gated Ca^{2+} channels plays an important role in control of neurotransmitter release from autonomic neurons (Hirning *et al.* 1988; Toth, Bindokas, Bleakman, Colmers & Miller, 1993), information about Ca^{2+} channels and their modulation in pelvic ganglion neurons might help us to understand the regulation of neuroeffector transmission in these neurons better. However, to our knowledge, there have been no studies which examine voltage-activated Ca^{2+} currents in male rat MPG neurons. Thus, the present study was undertaken to characterize the Ca^{2+} currents in MPG neurons of

* To whom correspondence should be addressed.

adult male rats and to correlate the electrophysiological data with the neurochemical phenotype as determined with histochemical and immuno-histochemical methods. Our data indicate that principal postganglionic autonomic neurons in the MPG of male rats contain at least two distinct subpopulations of neurons, i.e. adrenergic and non-adrenergic, which differ in morphology, Ca^{2+} channel expression and neurotransmitter modulation of Ca^{2+} channels.

METHODS

Neuron isolation

Single neurons of the major pelvic ganglia from male adult rats were enzymatically dispersed using a modification of the method previously described for rat superior cervical ganglion (Zhu & Ikeda, 1993). The rats were killed by decapitation with a laboratory guillotine and the major pelvic ganglia, located on the lateral surfaces of the prostate gland (Langworthy, 1965), were dissected out and placed in cold Hanks' balanced salt solution. The ganglia were then desheathed, cut into small pieces and incubated with 1·0 mg ml^{-1} collagenase type D (Boehringer Mannheim, Indianapolis, IN, USA), 0·1 mg ml^{-1} trypsin (Worthington, Freehold, NJ, USA), and 0·1 mg ml^{-1} DNAase Type I (Sigma Chemical Co., St Louis, MO, USA) in 10 ml of Earle's balanced salt solution at 35 °C for 1 h in a shaking water bath. After incubation, the ganglia were dissociated into single neurons by vigorous shaking of the flask containing the ganglia. The dispersed neurons were lightly pelleted by centrifugation at 50 *g* and then resuspended in Minimum Essential Medium (MEM) supplemented with 10% fetal calf serum, 1% glutamine and 1% penicillin–streptomycin solution (all from Life Technologies, Grand Island, NY, USA). The neurons were subsequently plated into 35 mm tissue culture dishes coated with poly-L-lysine and incubated in a humidified atmosphere containing 5% CO_2 in air at 37 °C. Neurons were used within 3–24 h of plating. Recordings were comparable during this time period.

Neuron staining

NADPH diaphorase (NADPHd) histochemical methods (Thomas & Pearse, 1964) were adapted from those previously described (Hope, Michael, Knigge & Vincent, 1991). Neurons were allowed to attach firmly to the culture substrate (> 2 h) and were then fixed with phosphate buffer (0·1 M, pH 7·4) containing 2% paraformaldehyde at room temperature (21–24 °C) for 30 min. Following fixation, the neurons were rinsed several times with Tris buffer (6·5 g l^{-1}, pH adjusted to 7·4 with HCl) and then incubated with Tris buffer containing 1 mg ml^{-1} Nitroblue Tetrazolium (Aldrich, Milwaukee, WI, USA), 0·4 mg ml^{-1} bNADPH (Sigma) and 0·3% Triton X-100 (Sigma) at 37 °C for 20–30 min. Subsequently, the reaction solution was replaced with Tris buffer and the neurons visualized with bright-field microscopy. NADPHd-positive neurons were stained an intense dark blue–purple colour. If β-NADPH was omitted from the reaction mixture, darkly stained neurons were absent.

TH-IR was detected immunohistochemically using a mouse (IgG2a) anti-TH monoclonal antibody (clone 2/40/15; Boehringer Mannheim) and a secondary antibody kit (Vectastain Elite ABC kit, Vector Laboratories, Burlingame, CA, USA) based on an avidin-biotin horseradish peroxidase complex (ABC). Briefly, plated neurons were fixed with 4% paraformaldehyde in sodium phosphate buffer (pH 7·2) for 15 min, washed three times (5 min) with phosphate-buffered saline (PBS) and incubated with blocking serum (horse serum, 15 μl ml^{-1} in PBS) for 15 min. Following overnight incubation at 4 °C with the primary antibody (4 ng μl^{-1} anti-TH antibody, 0·1% Tween 20 in PBS), the neurons were washed three times with PBS and processed according to the kit manufacturer's instructions. Neurons were incubated with secondary antibody and ABC reagent for 15 min, respectively. Following treatment with a diaminobenzidine-$NiCl_2$ (DAB substrate kit, Vector Laboratories), neurons were examined with bright-field microscopy for the dark gray–black peroxidase reaction product. Neurons treated identically except for omission of the primary antibody incubation step displayed no overt reaction product.

A computer-assisted video system was used to measure the diameter of stained and unstained neurons. For these studies, neurons were plated onto glass coverslips with individually labelled grids (Bellco, Vineland, NJ, USA) and visualized with bright-field microscopy using an inverted microscope. A field of dissociated neurons was first 'captured' (digitized) from a video image generated by a remote-head CCD camera with an 8-bit frame grabber card (QuickCapture, Data Translation, Marlboro, MA, USA) installed in a Macintosh II computer. An image analysis program (Image 1·44, Wayne Rasbund, NIH, Bethesda, MD, USA) was then used to determine the major and minor diameter of the neurons. The gridded coverslips allowed for the systematic scanning of the coverslip, thus avoiding the analysis of duplicate fields. Illumination was adjusted such that the dark precipitation products of the NADPHd and horseradish peroxidase (for TH-IR) reactions resulted in a modal pixel density near 255 (black). Neurons were considered stained in later analyses if the modal pixel density was 240 or greater. In practice, this analysis was equivalent to 'visual' determination of staining but was much more efficient, thus allowing greater numbers of neurons to be analysed. Generation and fitting (Gaussian functions) of mean cell diameter histograms was performed with the Macintosh program Igor (WaveMetrics, Lake Oswego, OR, USA). Objects smaller than 10 μm were excluded from all data sets in an attempt to restrict the analyses to principal postganglionic neurons (i.e. to exclude SIF cells and cellular debris).

Electrophysiology

The method for voltage clamping of single neurons using the whole-cell variant of patch-clamp technique (Hamill, Marty, Neher, Sakmann & Sigworth, 1981) has been described previously (Ikeda, 1991; Zhu & Ikeda, 1993). Patch electrodes were made from a borosilicate glass capillary (Corning 7052, Garner Glass Co., Claremont, CA, USA), coated with Sylgard 184 (Dow Corning, Midland, MI, USA), fire polished, and had resistances of 0·5–2 MΩ when filled with the solutions described below. The cell membrane capacitance and series resistance were determined with a small depolarizing pulse and then electronically compensated for (typically > 80%) using the Axopatch-1C patch-clamp amplifier (Axon Instruments, Foster City, CA, USA). Voltage-clamp protocols were generated by a Macintosh IIci computer using custom software. Traces were digitized at 200 μs per point and filtered at 2–5 kHz using the 4-pole Bessel filter in the clamp amplifier. All experiments were performed at room temperature (21–24 °C). Some neurons, after whole-cell recording, were subsequently examined for NADPHd reactivity or TH-IR. In these experiments, patch pipettes with a smaller opening (resistance of 2–4 MΩ) were used. Following recording (which was kept as brief as possible), the pipette was gently withdrawn from

the neuron and the location of the neuron marked by placing a scratch on the bottom of culture dish in the vicinity of the neuron.

Current traces were normally stored in the hard drive of the computer and later analysed using Igor. Current traces and current–voltage (I–V) relationships were corrected for linear leakage current as determined from hyperpolarizing pulses. Least squares non-linear regression estimate of Hill coefficients were performed with Igor curve-fitting functions. Results are presented as means ± S.E.M. unless otherwise stated. Student's paired or unpaired t tests were applied, as appropriate, to determine the statistical significance. The differences were considered significant if $P < 0.05$.

Solutions and drugs

For Ca^{2+} current recordings, the pipette solution contained (mM): 120 *N*-methyl-D-glucamine methanesulphonate (CH_3SO_3), 20 tetraethylammonium (TEA)-CH_3SO_3, 20 HCl, 11 ethyleneglycol-bis-(β-aminoethyl ether)*N,N,N′,N′*-tetraacetic acid (EGTA), 1 $CaCl_2$, 10 Hepes, 4 Mg-ATP, 0·3 Na_2-GTP, 14 creatine phosphate (Tris salt); pH 7·2 and 305 mosmol kg^{-1}. The external solution consisted of (mM): 145 TEA-CH3SO3, 10 Hepes, 10 $CaCl_2$, 15 glucose, 0·0005 TTX; pH 7·4 and 325 mosmol kg^{-1}. UK 14304 5-bromo-*N*-(4,5-dihydro-1H-imidazol-2-yl)-6-quinoxalinamine (Research Biochemicals Inc., Natick, MA, USA) a specific α_2-adrenergic agonist, was prepared from a 50 mM stock solution in 0·1 M HCl. ω-Conotoxin GVIA (ω-CgTX) was from Peninsula Labs (Belmont, CA, USA) and ω-agatoxin IVA (ω-Aga-IVA) was from Peptides International (Louisville, KY, USA). Drugs were applied to the neuron under study by rapidly lowering a large-bore (*ca* 10–15 μm tip diameter) micropipette (type N51A glass, Garner Glass Co.) containing the test solutions to within 10–20 μm of the cell. Drug application was terminated by lifting the pipette from the bathing medium.

RESULTS

Neurochemical phenotype of MPG neurons correlates with cell size

The major pelvic ganglion (MPG) of the male rat deviates from the general anatomical layout of the autonomic nervous system in that both parasympathetic and sympathetic postganglionic neuronal somata are situated within the same ganglion capsule (Dail, 1992). Results of previous studies (Dail *et al.* 1975; Keast & de Groat, 1989) have suggested that the neurochemical phenotype of MPG neurons (e.g. acetylcholinesterase-positive or TH-IR), as determined from tissue sections, correlates with neuron size. However, similar studies have not been conducted on enzymatically isolated neurons. Thus, experiments were undertaken to determine whether neurochemical phenotype, as determined from histochemical (NADPHd) and immunohistochemical (TH) methods, correlated with the size (mean somal diameter) of the dispersed MPG neurons.

A representative bright-field photomicrograph of dissociated MPG neurons stained for NADPHd, a marker (Dawson, Bredt, Fotuhi, Hwang & Snyder, 1991; Hope *et al.* 1991) for nitric oxide synthase (NOS), is shown in Fig. 1*A*. It is apparent that the dense formazan reaction product appears to be produced mainly in a subpopulation of smaller diameter neurons. Computer-assisted morphometric analysis of five separate neuron preparations (the number of neurons analysed per preparation ranged from 512 to 2426) confirmed that the somal diameter of NADPHd-positive neurons (22 ± 2 μm), which comprised 43 ± 3% of the neurons analysed, was significantly smaller ($P < 0.01$; Student's paired t test) than those of NADPHd-negative neurons (29 ± 2 μm). Somal diameters were determined from the arithmetic mean of the major and minor axis. Figure 1*B* depicts a histogram of NADPHd-positive neuron somal diameters from a single neuron preparation. The histogram was adequately described by a single Gaussian function (continuous line) with a mean of 18 μm. In contrast, a histogram of NADPHd-negative neurons (Fig. 1*C*) revealed a broad distribution of somal diameters with a sizeable fraction (*ca* 50%) of the subpopulation comprising large neurons (⩾30 μm). The histogram was adequately described (continuous line enclosing data) by a double Gaussian function with means of 22 and 34 μm.

A representative bright-field photomicrograph of dissociated MPG neurons stained for TH-IR is shown in Fig. 1*D*. When compared with Fig. 1*A*, it is apparent that neurons containing TH-IR comprise a subpopulation with larger somal diameters. Analysis of four separate neuron preparations (the number of neurons analysed per preparation ranged from 703 to 1376) revealed that the somal diameter of neurons with TH-IR (30 ± 1 μm), which comprised 42 ± 2% of the neurons analysed, was significantly ($P < 0.01$; Student's paired t test) larger than those neurons without TH-IR (22 ± 1 μm). Histograms of neurons with (Fig. 1*E*) and without (Fig. 1*F*) TH-IR were fit to single Gaussian function (continuous line) with means of 31 and 21 μm, respectively.

Ca^{2+} currents in MPG neurons

Ca^{2+} currents of single dissociated neurons from the rat MPG were recorded using the whole-cell variant of the patch-clamp technique in solutions designed to isolate Ca^{2+} currents. Preliminary studies revealed that low threshold T-type Ca^{2+} channels were present in some MPG neurons and appeared to be consistently present in the largest neurons in the preparation. As the morphometric data (Fig. 1) supported a correlation between neurochemical phenotype and neuron size, experiments were carried out to substantiate the relationship between expression of T-type Ca^{2+} channels and neuron size, and to explore whether the presence of T-type Ca^{2+} channels was restricted to a particular neurochemical phenotype.

The top and bottom panels of Fig. 2*A* depict superimposed currents traces from a representative large neuron (89 pF) displaying a T-type Ca^{2+} current component. Ca^{2+} currents were evoked from a holding potential of −90 mV with 70 ms depolarizing steps to various test pulse potentials. Between test pulse potentials of −50 and −20 mV, the step current inactivated relatively quickly (i.e. was transient)

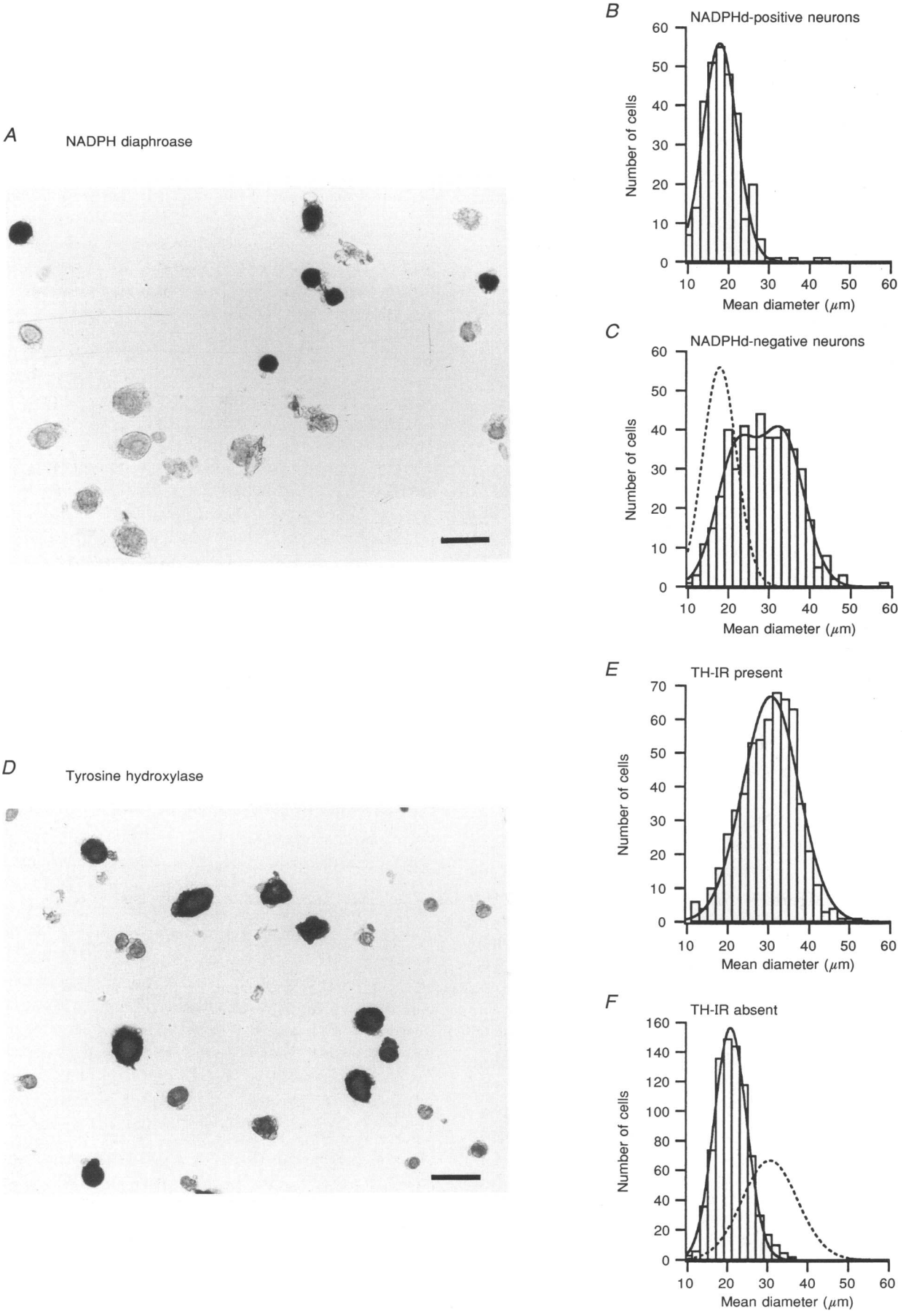

Figure 1. For legend see facing page.

and, following repolarization to the holding potential, a slowly decaying tail current resulting from Ca^{2+} channel deactivation was observed. Conversely, Ca^{2+} currents evoked from a holding potential of −60 mV inactivated very little during the 70 ms pulse and displayed a rapidly decaying tail current upon repolarization (Fig. 2*B*). Figure 2*C* illustrates current–voltage (*I–V*) relationships of Ca^{2+} currents recorded at holding potentials of −90 (●) and −60 mV (○), respectively. At the holding potential of −60 mV, the low threshold component of the Ca^{2+} current, evident in the inflection or 'hump' in the *I–V* relationship, was greatly attenuated and the maximal current amplitude was reduced. Figure 2*D* depicts the reversible block of the transient component of low threshold Ca^{2+} current by 500 μM amiloride, a relatively selective blocker of T-type Ca^{2+} channels (Tang, Presser & Morad, 1988). Mean inhibition by 500 μM amiloride in neurons expressing low threshold Ca^{2+} currents was 63·2 ± 5·3% ($n = 4$; determined at −40 mV). In neurons without overt T-type Ca^{2+} channels, 500 μM amiloride produced negligible block of the high threshold Ca^{2+} current (mean inhibition at 0 mV of −3·7 ± 2·7%, $n = 4$, data not shown). The mean $\tau_{inactivation}$ of the transient current component, as determined at −40 mV by fitting the decay phase to a single exponential plus a constant (i.e. a sustained component), was 45·8 ± 3 ms ($n = 3$). The sustained current component comprised about 25–33% of the total current at this voltage. The low threshold for activation, transient step current kinetics, retarded deactivation kinetics, attenuation by moderately depolarized (e.g. −60 mV) holding potentials and block by amiloride are consistent with previous descriptions of currents arising from T-type Ca^{2+} channels (Nowycky, Fox & Tsien, 1985; Matteson & Armstrong, 1986; Fox, Nowycky & Tsien, 1987; Tang *et al.* 1988).

Ca^{2+} currents from a representative medium-sized neuron (37 pF) in which no T-type Ca^{2+} channel component was observed is shown in Fig. 3. Superimposed families of current traces evoked from a holding potential of −90 mV are illustrated in Fig. 3*A*. No overt inward current was detected at test pulse potentials more hyperpolarized than −25 mV. Ca^{2+} currents evoked between −25 and −10 mV showed little inactivation during the 70 ms test pulse and tail currents decayed rapidly upon repolarization to holding potential. At a holding potential of −60 mV, the Ca^{2+} currents were nearly identical to those recorded at −90 mV except that the current amplitude was slightly decreased (Fig. 3*B* and *C*), possibly due to voltage-dependent inactivation.

As noted earlier, it was felt that larger neurons tended to possess a T-type Ca^{2+} current component more frequently than smaller neurons. To substantiate this impression, the neuron diameter, determined with a graduated reticule in the microscope eyepiece, and the membrane capacitance, a measure of cell surface area, were compared in neurons with and without and an overt T-type Ca^{2+} current component. As shown in Fig. 4*A*, most neurons without T-type Ca^{2+} channels were medium to small in size with a mean capacitance of 30 ± 2 pF (range, 10–52 pF; $n = 38$) and mean diameter of 23 ± 1 μm ($n = 32$). In contrast, neurons expressing T-type Ca^{2+} channels had a significantly greater ($P < 0·02$) mean capacitance (72 ± 8 pF; range, 27–127; $n = 33$) and diameter (34 ± 1 μm; $n = 31$) although the distribution of the two types of neurons overlapped considerably. Interestingly, the mean current density, as measured from the maximal current of the *I–V* curves, in neurons expressing T-type channels (40 ± 4 pA pF^{-1}; $n = 38$) was significantly less than that of neurons in which T-type channels were absent (78 ± 8 pA pF^{-1}, $n = 33$; $P < 0·01$).

Figure 1. NADPH diaphorase (NADPHd) histochemistry and tyrosine hydroxylase (TH) immunohistochemistry of dissociated major pelvic ganglion (MPG) neurons

A, bright-field photomicrograph of enzymatically dissociated MPG neurons following fixation and staining for NADPHd. Note that the NADPHd-positive cells (darker) are generally of smaller diameter when compared to unreactive neurons. Calibration bar represents 50 μm. *B*, histogram of somal diameters from 298 NADPHd-positive neurons. The solid line represents the best fit to a Gaussian function with mean and standard deviation (S.D.) of 18·0 and 5·9 μm, respectively. *C*, histogram of somal diameters from 460 NADPHd-negative neurons. The continuous line represents the best fit to a double Gaussian function with means of 22·2 and 33·7 μm and S.D. values of 7·2 and 7·3 μm, respectively. The dashed line represents the fit of the histogram depicted in *B* superimposed for comparison. Neurons in *B* and *C* are from the same preparation. NADPHd-positive neurons comprised 39% (298 out of 758) of the total population in this preparation. *D*, bright-field photomicrograph of MPG neurons following fixation and staining for TH-IR. Note that the cells displaying TH-IR (darker) were generally of larger diameter when compared to unreactive neurons. Calibration bar represents 50 μm. *E*, histogram of somal diameters from 574 neurons with TH-IR. The continuous line represents the best fit of a Gaussian function to the data with mean and S.D. of 30·7 and 9·7 μm, respectively. *F*, histogram of somal diameters from 802 neurons without TH-IR. The continuous line represents the best fit to a Gaussian function with a mean and S.D. of 20·8 and 5·7 μm, respectively. The dashed line represents the fit of the histogram depicted in *D* superimposed for comparison. Neurons in *D* and *E* are from the same preparation. Neurons with TH-IR comprised 42% (573 out of 1376) of the total population in this preparation.

Neurochemical phenotype of MPG neurons expressing T-type Ca^{2+} channels

As both the neurochemical phenotype and presence of T-type Ca^{2+} channels correlated with neuron size, it was hypothesized that neurochemical phenotype might be associated with the presence or absence of T-type Ca^{2+} channels. To test this hypothesis, Ca^{2+} currents were recorded from neurons which were subsequently marked (by scratching the dish in the vicinity of the neuron) for later identification and processed for NADPHd activity or TH-IR as described above (Fig. 1). As illustrated in Fig. 4*B*, none of the neurons (0 out of 7) displaying T-type Ca^{2+} channels were NADPHd-positive whereas about 57% of the neurons (4 out of 7) without overt T-type Ca^{2+} channels stained positively for NADPHd. Conversely, 100% of the neurons (13 out of 13) without overt T-type Ca^{2+} channels

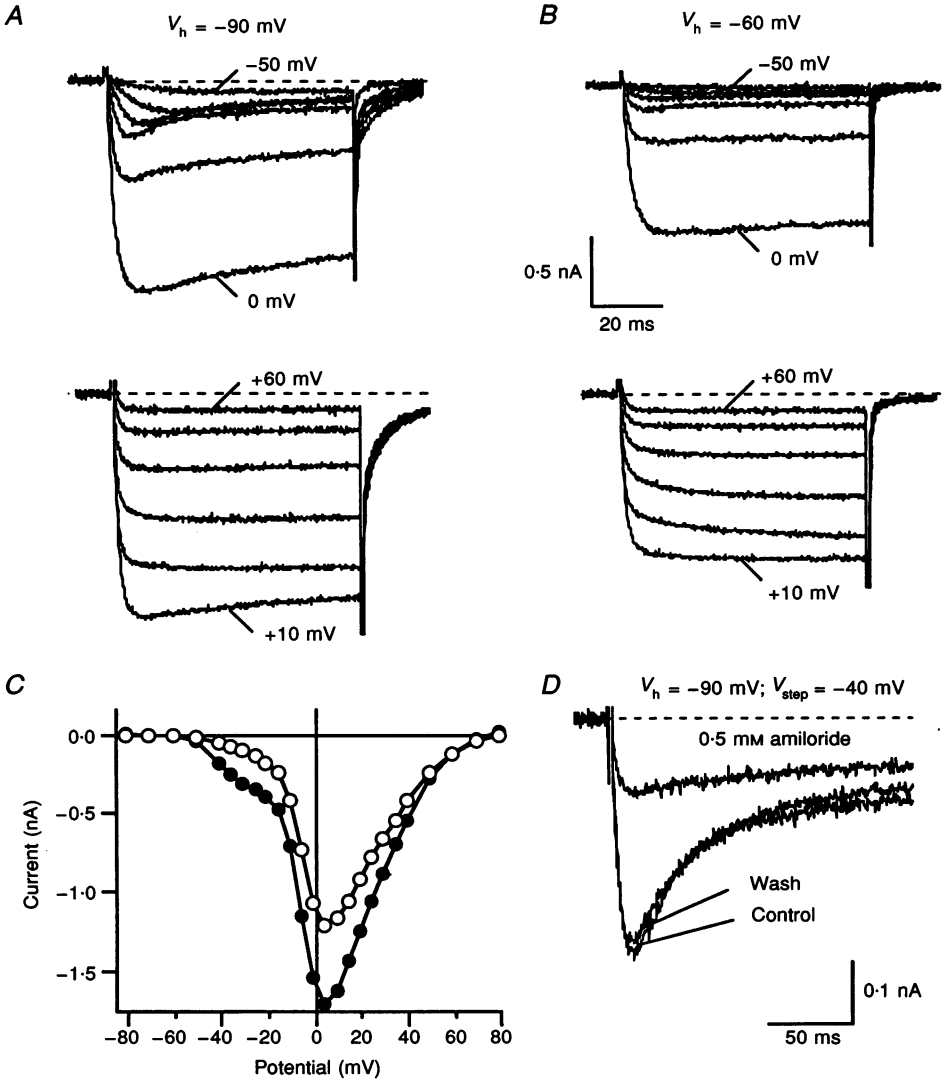

Figure 2. Whole-cell Ca^{2+} currents in neurons expressing both low and high threshold Ca^{2+} channels

A, Ca^{2+} channel currents evoked by 70 ms pulses from a holding potential of −90 mV to various test potentials (up to +80 mV). The top and bottom set of superimposed traces depict currents resulting from depolarizations to potentials between −50 and 0 mV, and +10 and +60 mV, respectively, in 10 mV increments. Note the transient step currents between −40 and −20 mV and the slowly decaying tail currents. *B*, superimposed current traces, from the same neuron shown in *A*, evoked from a holding potential of −60 mV. Calibration applies to traces in both *A* and *B*. *C*, the current–voltage (*I–V*) relationship of Ca^{2+} currents recorded at holding potentials of −90 mV (●) and −60 mV (○). The current amplitudes were determined isochronally 10 ms after each test pulse from the traces shown in *A* and *B*. *D*, superimposed current traces evoked by a step to −40 mV from a holding potential of −90 mV in a different neuron from that shown in *A–C*. Traces obtained in the absence, presence and during washout of 500 μM amiloride.

isplayed no TH-IR whereas 100% of the neurons (15 out of 15) expressing T-type Ca^{2+} channels contained TH-IR (Fig. 4*C*). One neuron (68 pF) expressed an atypical Ca^{2+} current component which could not be positively attributed to T-type Ca^{2+} channels, i.e. the step current was not transient but a slow tail current was observed upon repolarization. This neuron did not contain TH-IR and was not included in Fig. 4*C*. These data show that (1) all neurons expressing T-type Ca^{2+} channels contain TH-IR, and are thus adrenergic and presumably sympathetic, (2) all neurons expressing T-type Ca^{2+} channels were NADPHd-negative, (3) all neurons without T-type Ca^{2+} currents were non-adrenergic (i.e. lacked TH-IR) and (4) about half of the neurons without overt T-type Ca^{2+} channels were NADPHd-positive.

Contribution of high threshold L-, N- or P-type Ca^{2+} channels

At least four different Ca^{2+} channels (T-, L-, N- and P-types) have been identified in neurons based on electrophysiological and pharmacological criteria (Nowycky *et al.* 1985; Fox *et al.* 1987; Mintz, Venema, Swiderek, Lee, Bean & Adams, 1992). The contribution of high threshold Ca^{2+} channel types to the whole-cell currents was investigated using nifedipine, a dihydropyridine (DHP) L-type channel blocker, ω-CgTX, an N-type channel blocker, and ω-Aga-IVA, a P-type channel blocker. Figure 5*A* illustrates the protocol used to determine the relative inhibition of whole-cell Ca^{2+} current by these three blockers. In a neuron held at −60 mV to inactivate T-type Ca^{2+} currents, the majority of whole-cell Ca^{2+} current arose from N-type Ca^{2+} currents as 10 μM ω-CgTX inhibited the Ca^{2+} current by about 60% (Fig. 5*A* and *B*). No contribution of P-type Ca^{2+} channels was detected based on the minimal effect of 0·2 μM ω-Aga-IVA application. A small contribution from the L-type Ca^{2+} channels was demonstrated by an 11% inhibition induced by 10 μM nifedipine (Fig. 5*A* and *B*). About 30% of the total current was not sensitive to any of these blockers and represents an as yet undefined Ca^{2+} current component. The existence of L-type Ca^{2+} channels in MPG neurons was further substantiated by application of (+)202-791 (2 μM), a DHP Ca^{2+} channel 'agonist' (data

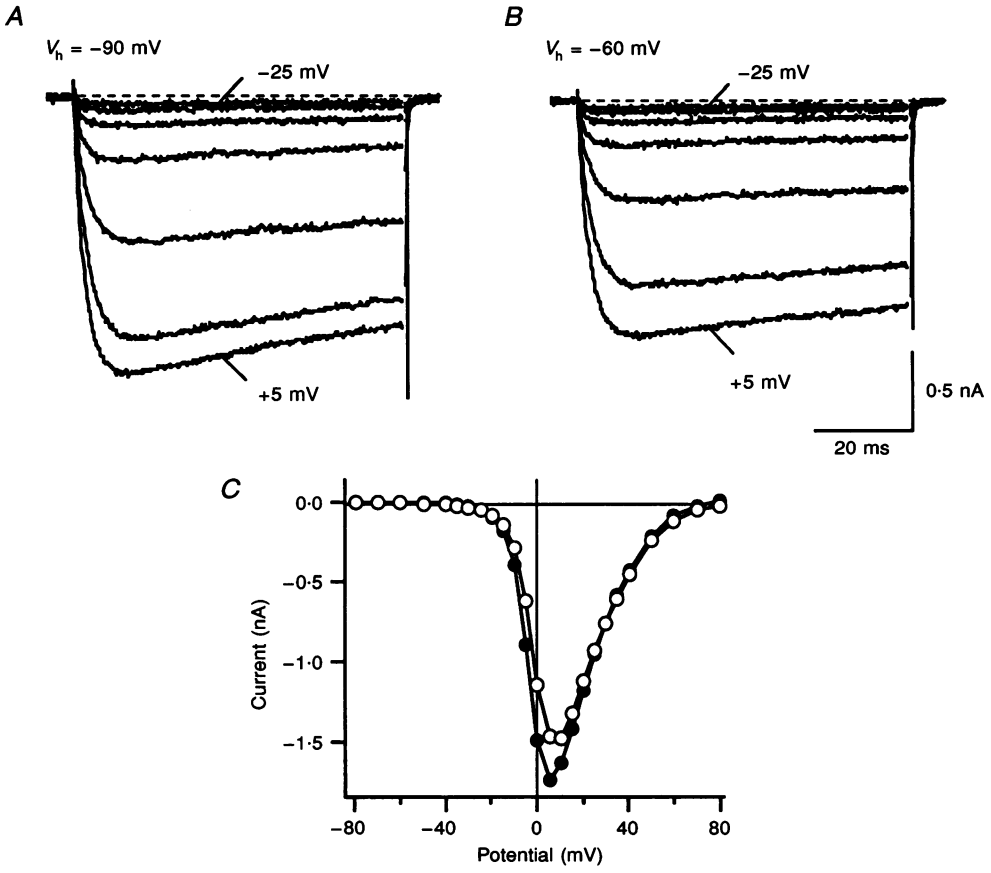

Figure 3. Whole-cell Ca^{2+} currents in a neuron expressing only high threshold Ca^{2+} channels

A, superimposed Ca^{2+} current traces evoked from a holding potential of −90 mV by a series of 70 ms test pulse to potentials between −25 and +5 mV (5 mV increments). Note the absence of a slow tail current component (cf. Fig. 2*A*) *B*, superimposed current traces recorded as in *A* but from a holding potential of −60 mV. *C*, *I–V* relationships of Ca^{2+} currents recorded from holding potentials of −90 mV (●) and −60 mV (○). Data shown in *A–C* were from the same neuron.

not shown). In the presence of (+)202-791, the voltage at which maximal current amplitude was attained was shifted about 10 mV hyperpolarized, maximal current amplitude was increased by about 23% and a slowly decaying tail current was observed (Plummer, Logothetis & Hess, 1989; Ikeda, 1991).

Figure 5*C* summarizes the mean inhibition of whole-cell Ca^{2+} currents by various agents in neurons with (filled bar) or without (open bar) T-type Ca^{2+} channels. These data demonstrate that (1) N-type Ca^{2+} channels accounted for the majority of the whole-cell currents (62–69%), (2) the contribution from P-type channels was negligible, (3) a small contribution arising from DHP-sensitive L-type Ca^{2+} channels was detectable and (4) no significant differences in the relative contribution of N- or L-type Ca^{2+} channels to the total Ca^{2+} current was observed when the neurons were subdivided based on presence or absence of T-type Ca^{2+} channels.

Calcium channel modulation by α_2-adrenoreceptors

Ca^{2+} channels in sympathetic (Hille, 1994) and parasympathetic (Xu & Adams, 1993) neurons are highly modulated by various neurotransmitters and neuromodulators. Experiments were carried out to determine whether Ca^{2+} channels were differentially modulated by α_2-adrenoceptors in MPG neurons with and without T-type Ca^{2+} channels. Figure 6*A* shows the Ca^{2+} current inhibition induced by sequential application of increasing concentrations (0·1–50 μM) of UK 14304, a specific α_2-adrenoceptor agonist, to a neuron expressing T-type current. UK 14304 applications induced a concentration-dependent inhibition (Fig. 6*A*) and changed the step current kinetics to a slowly rising trajectory (Fig. 6*B*). The slow tail current, representing primarily the T-type Ca^{2+} channel deactivation, was not significantly affected by application of 1 μM UK 14304 (Fig. 6*B*). In contrast, similar applications of UK 14304 to a neuron displaying no overt T-type Ca^{2+} channels produced a relatively weak Ca^{2+} current inhibition (Fig. 6*C* and *D*). Figure 6*E* summarizes the concentration–response relationships for mean Ca^{2+} current inhibition produced by UK 14304. For neurons expressing T-type Ca^{2+} channels, UK 14304 produced a maximal inhibition of 60 ± 1% ($n = 6$) and a half-maximal block at 0·1 μM, as determined from fits of the data to a single-site binding isotherm. In contrast, for neurons without overt T-type Ca^{2+} channels, UK 14304 produced a maximal inhibition of only 27 ± 4% ($n = 6$) and a half-maximal block at 0·6 μM.

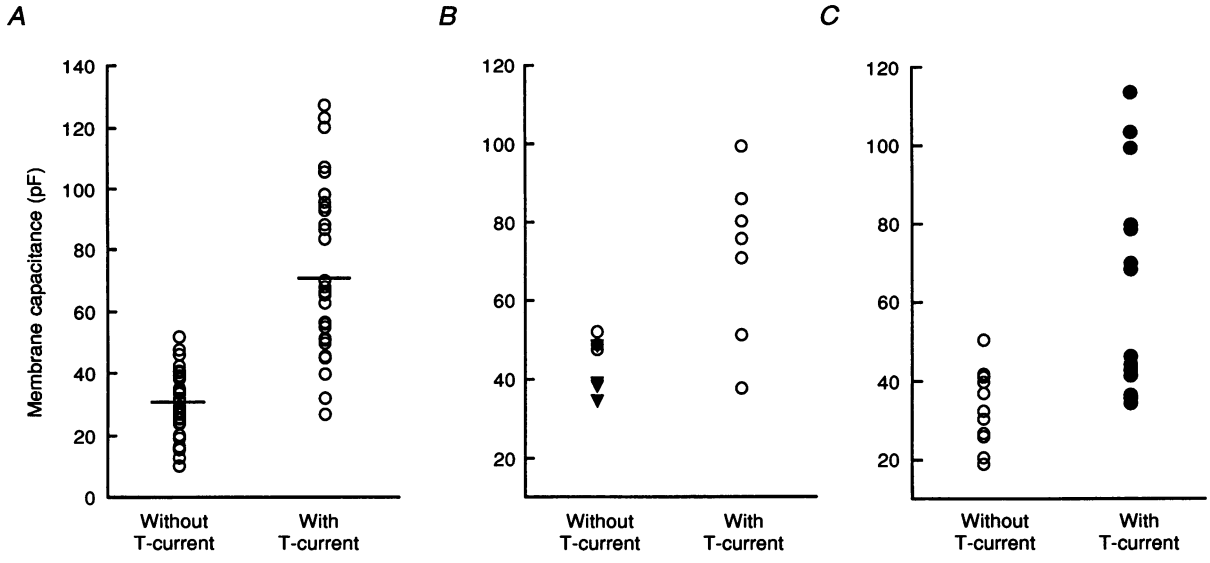

Figure 4. Comparison of membrane capacitance, NADPHd reactivity and TH-IR in MPG neurons

Neurons were divided into two subpopoulations based on the presence or absence of T-type Ca^{2+} currents and displayed as scatter plots. Membrane capacitance (C_m) was determined from numerical integration of transients elicited with a 10 mV depolarizing pulse prior to electronic compensation of C_m. *A*, neurons displaying T-type Ca^{2+} channels had a greater mean C_m and broader range of C_m values. Horizontal bars indicate the mean C_m for each group. *B*, NADPHd reactivity and Ca^{2+} currents determined in the same neurons. After recording Ca^{2+} currents, the patch pipette was carefully removed and the location of a neuron marked by placing a scratch on the bottom of the culture dish. Subsequently, identified neurons were processed and scored for the absence (○) or presence (▼) of NADPHd reactivity. *C*, TH-IR and Ca^{2+} currents determined in the same neurons. After recording Ca^{2+} currents, the patch pipette was carefully removed and the location of a neuron marked as in *B*. Subsequently, identified neurons were processed and scored for the absence (○) or presence (●) of TH-IR.

DISCUSSION

Adrenergic and non-adrenergic neurons in the rat MPG

The morphometric data on dispersed MPG neurons (Fig. 1) showed that at least two discrete subpopulations of MPG neurons reside within the MPG as determined from neurochemical phenotype. If TH-IR is accepted as a marker for adrenergic (and hence sympathetic) neurons, then about 40% of the total neurons isolated were adrenergic neurons. Adrenergic neurons had a larger mean diameter, about 30 μm, when compared with non-adrenergic neurons (about 20 μm). Because of the overlap in subpopulations (Fig. 1*F*), somal diameter would be a poor predictor of adrenergic *versus* non-adrenergic phenotype unless the extremes of the two subpopulations were used. Thus, neurons greater than 30–35 μm in diameter are likely (>90%) to be adrenergic while those less than 18–20 μm are likely to be non-adrenergic. The data obtained from dispersed neurons compares favourably with previous studies of tissue sections which show that neurons with TH-IR comprise (1) 40–60% of the neurons in male rat MPG (Karhula, Soinila & Häppölä, 1993), and (2) a subpopulation of larger neurons (Dail, Minorsky, Moll & Manzanares, 1986; Keast & de Groat, 1989) as determined from mean somal diameter (34·2 μm) or surface area (1015 μm^2). In addition, MPG neurons of male rats which stain positively for acetylcholinesterase (AChE; Dail *et al.* 1975), VIP (Keast & de Groat, 1989) or NADPHd (Keast, 1992) markers for non-adrenergic (possibly parasympathetic) neurons, have mean somal diameters of about 20–25 μm, consistent with the non-adrenergic subpopulation of neurons reported here. The question then arises as to what proportion of non-adrenergic neurons are cholinergic. Unfortunately, most antibodies against choline acetyltransferase (ChAT), a marker for cholinergic neuronal systems, do not stain postganglionic parasympathetic neurons (Dail & Hamill, 1989). Thus, the resolution of this question awaits the availability of antibodies which readily recognize the ChAT isoform found in parasympathetic

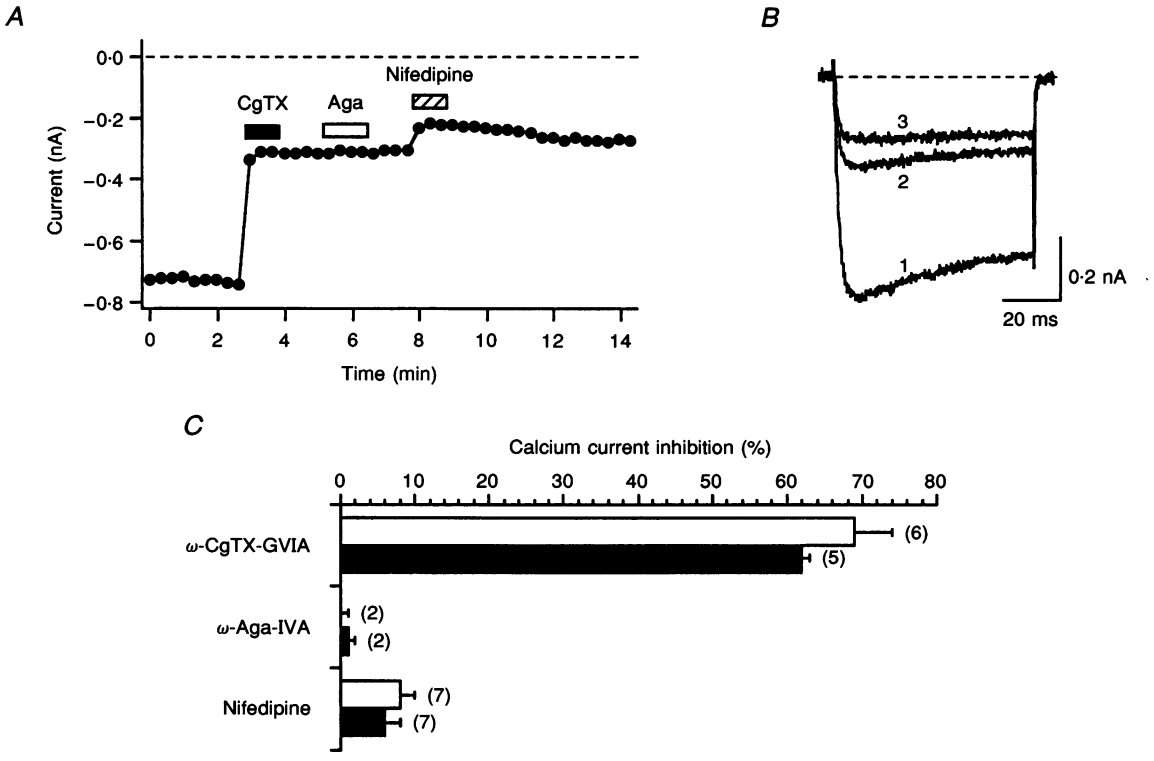

Figure 5. Contribution of high threshold L-, N- and P-type channels to the whole-cell current

A, time course of current amplitudes determined from Ca^{2+} currents evoked every 20 s by a depolarizing test pulse to +10 mV from a holding potential of −60 mV. The current amplitudes were determined isochronally 10 ms after the start of the test pulse. Sequential application of test solutions containing 10 μM ω-CgTX, 0·2 μM ω-Aga-IVA and 10 μM nifedipine are indicated by the filled bar, open bar and hatched bar, respectively. *B*, superimposed current traces recorded under the control conditions (1) and during application of ω-CgTX (2) or nifedipine (3) from the neuron shown in *A*. *C*, summary of Ca^{2+} current inhibition produced by 10 μM ω-CgTX , 0·2 μM ω-Aga-IVA and 10 μM nifedipine in neurons with (filled bars) or without (open bars) overt T-type Ca^{2+} channels. Inhibition was measured as in *A* (holding potential of −60 mV). The presence of T-type Ca^{2+} channels was determined from a holding potential of −90 mV.

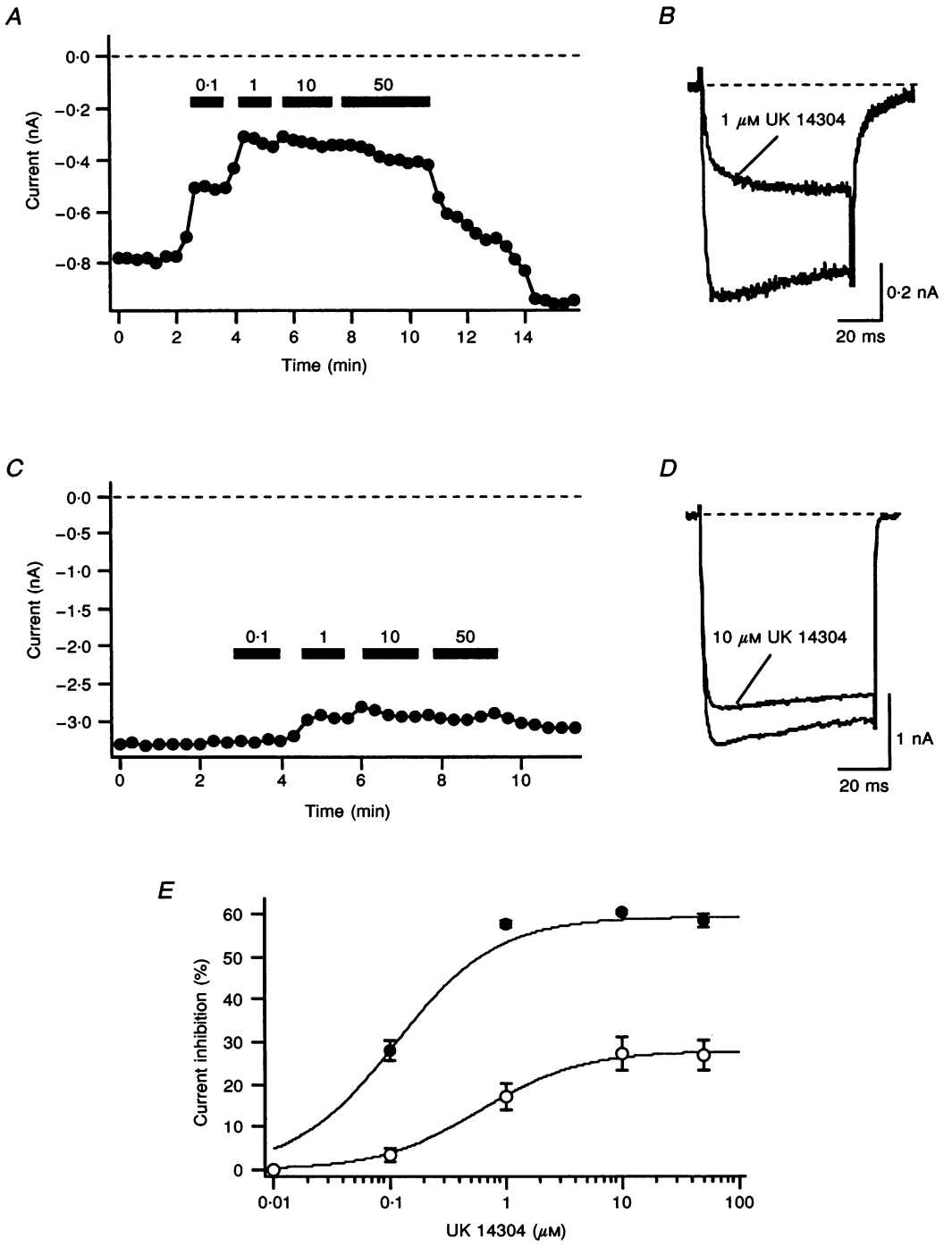

Figure 6. Differential modulation of Ca^{2+} channels by α_2-adrenoceptors

A, time course of Ca^{2+} current inhibition during sequential applications of increasing concentrations (bars) of UK 14304, an α_2-adrenoceptor agonist, in a neuron expressing T-type Ca^{2+} channels. Ca^{2+} currents were elicited as in Fig. 5*A* but from a holding potential of −80 mV. *B*, superimposed current traces recorded in the absence (lower traces) and presence (upper traces) of 1 μM UK 14304. Data in *A* and *B* are from the same neuron. Note that the slow tail current was not affected by UK 14304. *C*, time course of Ca^{2+} current amplitude, determined as in *A*, from a neuron without an overt T-type Ca^{2+} channel component during sequential applications of UK 14304. *D*, superimposed current traces recorded in the absence and presence of 10 μM UK 14304. Data in *C* and *D* are from the same neuron. *E*, concentration–response curves (mean ± S.E.M.) of high threshold Ca^{2+} current inhibition produced by UK 14304 from MPG neurons with (●, $n = 6$) or without (○, $n = 6$) T-type Ca^{2+} channel current components. The continuous lines represent the best fit of a single-site binding isotherm to the data as determined from non-linear regression analysis.

neurons. Finally, non-adrenergic neurons in pelvic ganglion of female rats appear to be relatively large (Kanerva, Lietzén & Teräväinen, 1972) when compared to adrenergic neurons and thus size relationships cannot be extrapolated to a homologous ganglion, even within a single species.

NADPHd activity, a marker for NOS (but see below), was found in a subpopulation of smaller MPG neurons with a similar mean diameter and distribution as the non-adrenergic neurons (cf. Fig. 1*B* and *F*). These data are consistent with studies which demonstrate that MPG neurons innervating penile erectile tissue (as determined from retrograde labelling) comprise a relatively homogenous subpopulation of small (15–20 μm) neurons which stain positively for AChE, NADPHd and VIP-IR, and negatively for TH-IR (Dail *et al.* 1986; Keast & de Groat, 1989; Keast, 1992; Vizzard, Erdman, Förstermann & de Groat, 1994). Thus, most, if not all, NADPHd-positive neurons are non-adrenergic. However, it is likely that NADPHd-positive neurons are a subset of non-adrenergic neurons as suggested by the broad distribution of NADPHd-negative neurons (cf. Fig. 1*C* and *F*). It should be noted that NADPHd staining and NOS-IR in rat MPG neurons may not identify an identical subpopulation of neurons (Vizzard *et al.* 1994). Thus, whether NADPHd activity is a reliable marker for NOS in MPG neurons, as it appears to be for most neurons (Dawson *et al.* 1991; Hope *et al.* 1991), remains to be determined.

T-type Ca^{2+} channels as a marker for adrenergic neurons in the MPG

The presence of low threshold T-type Ca^{2+} channels in a subpopulation of neurons from the male rat MPG was unexpected as most studies of rat autonomic neurons report that the whole-cell Ca^{2+} current arises exclusively from high threshold Ca^{2+} channels. Whole-cell recordings of Ca^{2+} currents from neurons of rat paravertebral (Marrion, Smart & Brown, 1987; Schofield & Ikeda, 1988; Plummer, Logothetis & Hess, 1989; Chen & Schofield, 1993) and prevertebral (Carrier & Ikeda, 1992) sympathetic neurons, as well as parasympathetic neurons (Aibara, Ebihara & Akaike, 1992; Xu & Adams, 1992), fail to reveal a low threshold Ca^{2+} current component. However, in rabbit vesical parasympathetic ganglia 36% of the neurons display T-type Ca^{2+} channels (Akasu, Tsurusaki & Tokimasa, 1990), suggesting that this phenomenon may be peculiar to autonomic neurons innervating pelvic structures.

Interestingly, our data revealed that the expression of T-type Ca^{2+} channels was restricted solely to adrenergic neurons. This relationship was first suspected from the perceived association of T-type Ca^{2+} channels with large capacitance neurons (Fig. 4*A*) and confirmed by performing voltage-clamp recordings and TH immunohistochemistry on the same neurons (Fig. 4*C*). Similar experiments showed that neurons expressing T-type Ca^{2+} channels were NADPHd negative. About half of the neurons without overt T-type Ca^{2+} channels were NADPHd positive, corroborating the interpretation that NADPHd-positive neurons comprise a subset of non-adrenergic neurons in rat MPG. Taken together, these data indicate that the presence or absence of T-type Ca^{2+} channels is a reliable electrophysiological marker for neurons with adrenergic and non-adrenergic phenotype, respectively. As T-type Ca^{2+} channels are readily identified without the use of pharmacological agents from their unique biophysical properties, namely low threshold for activation, transient step current kinetics, relatively hyperpolarized half-inactivation voltage and slow tail current kinetics (Nowycky *et al.* 1985; Matteson & Armstrong, 1986; Fox *et al.* 1987), the use of this criteria for discriminating adrenergic from non-adrenergic neurons in the rat MPG should provide a rapid and convenient method for studying phenotype-specific Ca^{2+} channel properties (see below) of male rat MPG neurons.

Although the physiological role subserved by T-type Ca^{2+} channels in rat MPG ganglion neurons is unknown, the presence of these channels in adrenergic neurons may be a clue that these neurons possess unique properties. In this regard, the adrenergic neurons in pelvic ganglia have been reported to differ from other sympathetic neurons in that the target organs innervated lie in close proximity to the postganglionic neurons. Moreover, these 'short' adrenergic neurons exhibit a number of physiological and pharmacological properties which differentiate them from conventional 'long' adrenergic neurons. For example, 'short' adrenergic neurons are reported to be more resistant to the noradrenaline-depleting properties of reserpine when compared with neurons of paravertebral ganglia (Owman, Alm & Sjöberg, 1983).

High threshold Ca^{2+} channels and modulation

By dividing neurons into subpopulations with and without T-type Ca^{2+} channels, it was possible to compare, using pharmacological agents, the contribution of different Ca^{2+} channel subtypes contributed to the high threshold Ca^{2+} current in adrenergic and non-adrenergic neurons. Based on Ca^{2+} current inhibition produced by application of ω-CgTX-GVIA, ω-Aga-IVA and nifedipine, it was concluded that N-type Ca^{2+} channels underlie the majority (60–70%) of high threshold Ca^{2+} current in both type of neurons while P- and L-type Ca^{2+} channels contribute less than 10% of the current. Approximately 20–25% of the high threshold Ca^{2+} current was not blocked by any of these agents. The profile of high threshold Ca^{2+} channel subtypes present in adrenergic and non-adrenergic neurons appeared to be similar (Fig. 5*C*).

In contrast, modulation of high threshold Ca^{2+} channels by α_2-adrenoreceptor stimulation with UK 14304 was markedly different in adrenergic and non-adrenergic neurons (based on presence or absence of T-type Ca^{2+} channels). Maximal inhibition of high threshold Ca^{2+}

current was much greater in adrenergic neurons and reminiscent of the block of N-type Ca^{2+} channels produced by a number neurotransmitters in rat superior cervical ganglion neurons (Ikeda & Schofield, 1989; Ikeda, 1992; Zhu & Ikeda, 1993). T-type Ca^{2+} channels did not appear to be modulated by α_2-adrenoreceptors based on the lack of effect of UK 14304 on the slow tail current component (Fig. 6*B*). The efficacy of high threshold Ca^{2+} channel modulation by α_2-adrenoreceptor in adrenergic MPG neurons is consonant with the idea that autoreceptors play an important role in regulating neurotransmitter release from sympathetic nerve terminals (Hirning *et al.* 1988; Toth *et al.* 1993). Conversely, Ca^{2+} channels of non-adrenergic neurons in the rat MPG were less sensitive to inhibition mediated by α_2-adrenoceptors. The relatively weak response to UK 14304 in the present study may result from a low density of α_2-adrenoreceptors, G-proteins, or poor coupling between receptors and effectors. Regardless of the mechanism, these results suggest that the factors controlling neurotransmitter phenotype influence both Ca^{2+} channel subtype expression and modulation.

Conclusions

In conclusion, our data indicate that principal post-ganglionic autonomic neurons in the MPG of male rats contain at least two distinct subpopulations of neurons. Neurons with an adrenergic phenotype (based on TH-IR), and thus presumably sympathetic, were larger, expressed T-type Ca^{2+} channels and were highly modulated by α_2-adrenoceptors. Conversely, neurons with a non-adrenergic phenotype, and thus possibly parasympathetic, were smaller, displayed no overt T-type Ca^{2+} channel component and were weakly modulated by α_2-adrenoceptors. We propose that the presence or absence of T-type Ca^{2+} channels provides a rapid and convenient predictor of adrenergic or non-adrenergic phenotypes, respectively, in MPG neurons.

Aibara, K., Ebihara, S. & Akaike, N. (1992). Voltage-dependent ionic currents in dissociated paratracheal ganglion cells of the rat. *Journal of Physiology* **457**, 591–610.

Akasu, T., Tsurusaki, M. & Tokimasa, T. (1990). Reduction of the N-type calcium current by noradrenaline in neurones of rabbit vesical parasympathetic ganglia. *Journal of Physiology* **426**, 439–452.

Carrier, G. O. & Ikeda, S. R. (1992). TTX-sensitive Na^+ channels and Ca^{2+} channels of the L- and N-type underlie the inward current in acutely dispersed coeliac-mesenteric ganglia neurons of adult rats. *Pflügers Archiv* **421**, 7–16.

Chen, C. & Schofield, G. G. (1993). Differential modulation of calcium currents by norepinephrine in rat sympathetic neurons. *Journal of Neurophysiology* **70**, 1440–1450.

Dail, W. G. (1992). Autonomic innervation of male reproductive genitalia. In *The Autonomic Nervous System*, vol. 2, *Nervous Control of the Urogenital System*, ed. Maggi, C. A., pp. 69–101. Harwood Academic Publishers, London.

Dail, W. G., Evan, A. P. & Eason, H. R. (1975). The major ganglion in the pelvic plexus of the male rat. A histochemical and ultrastructural study. *Cell and Tissue Research* **159**, 49–62.

Dail, W. G. & Hamill, R. W. (1989). Parasympathetic nerves in penile erectile tissue of the rat contain choline acetyltransferase. *Brain Research* **487**, 165–170.

Dail, W. G., Minorsky, N., Moll, M. A. & Manzanares, K. (1986). The hypogastric nerve pathway to penile erectile tissues: histochemical evidence supporting a vasodilator role. *Journal of the Autonomic Nervous System* **15**, 341–349.

Dawson, T. M., Bredt, D. S., Fotuhi, M., Hwang, P. M. & Snyder, S. H. (1991). Nitric oxide synthase and neuronal NADPH diaphorase are identical in brain and peripheral tissues. *Proceedings of the National Academy of Sciences of the USA* **88**, 7797–7801.

de Groat, W. C. & Booth, A. M. (1992). Neural control of penile erection. In *The Autonomic Nervous System*, vol. 2, *Nervous Control of the Urogenital System*, ed. Maggi, C. A., pp. 467–524. Harwood Academic Publishers, London.

de Groat, W. C., Booth, A. M. & Yoshimura, N. (1992). Neurophysiology of micturation and its modification in animal models of human disease. In *The Autonomic Nervous System*, vol. 2, *Nervous Control of the Urogenital System*, ed. Maggi, C. A., pp. 227–290. Harwood Academic Publishers, London.

Fox, A. P., Nowycky, M. C. & Tsien, R. W. (1987). Kinetic and pharmacological properties distinguishing three types of calcium currents in chick sensory neurones. *Journal of Physiology* **394**, 149–172.

Giuliano, F., Rampin, O., Schirar, A., Jardin, A. & Rousseau, J. P. (1993). Autonomic control of penile erection: modulation by testosterone in the rat. *Journal of Neuroendocrinology* **5**, 677–683.

Hamill, O. P., Marty, A., Neher, E., Sakmann, B. & Sigworth, F. J. (1981). Improved patch-clamp techniques for high-resolution current recording from cells and cell-free membrane patches. *Pflügers Archiv* **391**, 85–100.

Hille, B. (1994). Modulation of ion-channel function by G-protein-coupled receptors. *Trends in Neurosciences* **17**, 531–536.

Hirning, L. D., Fox, A. D., McCleskey, E. W., Olivera, B. M., Thayer, S. A., Miller, R. J. & Tsien, R. W. (1988). Dominant role of N-type Ca^{2+} channels in evoked release of norepinephrine from sympathetic neurons. *Science* **239**, 57–61.

Hope, B. T., Michael, G. J., Knigge, K. M. & Vincent, S. R. (1991). Neural NADPH diaphorase is a nitric oxide synthase. *Proceedings of the National Academy of Sciences of the USA* **88**, 2811–2814.

Ikeda, S. R. (1991). Double-pulse calcium channel current facilitation in adult rat sympathetic neurones. *Journal of Physiology* **439**, 181–214.

Ikeda, S. R. (1992). Prostaglandin modulation of Ca^{2+} channels in rat sympathetic neurones is mediated by guanine nucleotide binding proteins. *Journal of Physiology* **458**, 339–359.

Ikeda, S. R. & Schofield, G. G. (1989). Somatostatin blocks a calcium current in rat sympathetic ganglion neurones. *Journal of Physiology* **409**, 221–240.

Kanerva, L., Lietzén, R. & Teräväinen, H. (1972). Catecholamines and cholinesterases in the paracervical (Frankenhäuser) ganglion of normal and pregnant rats. *Acta Physiologica Scandinavica* **86**, 271–277.

KARHULA, T., SOINILA, S. & HÄPPÖLÄ, O. (1993). Comparison of immunohistochemical localization of [Met^5] enkephalin-Arg^6-Gly^7-Leu^8, vasoactive intestinal polypeptide and tyrosine hydroxylase in the major pelvic ganglion of the rat. *Neuroscience* **54**, 253–261.

KEAST, J. R. (1992). A possible neural source of nitric oxide in the rat penis. *Neuroscience Letters* **143**, 69–73.

KEAST, J. R. & DE GROAT, W. C. (1989). Immunohistochemical characterization of pelvic neurons which project to the bladder, colon, or penis in rats. *Journal of Comparative Neurology* **288**, 387–400.

LANGWORTHY, O. R. (1965). Innervation of the pelvic organs of the rat. *Investigative Urology* **2**, 491–511.

MARRION, N. V., SMART, T. G. & BROWN, D. A. (1987). Membrane currents in adult rat superior cervical ganglia in dissociated tissue culture. *Neuroscience Letters* **77**, 55–60.

MATTESON, D. R. & ARMSTRONG, C. M. (1986). Properties of two types of calcium channels in clonal pituitary cells. *Journal of General Physiology* **87**, 161–182.

MILLS, T. M., WIEDMEIER, V. T. & STOPPER, V. S. (1992). Androgen maintenance of erectile function in the rat penis. *Biology of Reproduction* **46**, 342–348.

MINTZ, I. M., VENEMA, V. J., SWIDEREK, K. M., LEE, T. D., BEAN, B. P. & ADAMS, M. E. (1992). P-type calcium channels blocked by the spider toxin omega-Aga-IVA. *Nature* **355**, 827–829.

NOWYCKY, M. C., FOX, A. P. & TSIEN, R. W. (1985). Three types of neuronal calcium channel with different calcium agonist sensitivity. *Nature* **316**, 440–443.

OWMAN, C., ALM, P. & SJÖBERG, N.-O. (1983). Pelvic autonomic ganglia: Structure, transmitters, function and steroid influence. In *Autonomic Ganglia*, ed. ELFVIN, L.-G., pp. 125–143. John Wiley & Sons, Ltd, New York.

PLUMMER, M. R., LOGOTHETIS, D. E. & HESS, P. (1989). Elementary properties and pharmacological sensitivities of calcium channels in mammalian peripheral neurons. *Neuron* **2**, 1453–1463.

SCHOFIELD, G. G. & IKEDA, S. R. (1988). Sodium and calcium currents of acutely isolated adult rat superior cervical ganglion neurons. *Pflügers Archiv* **411**, 481–490.

TANG, C.-M., PRESSER, F. & MORAD, M. (1988). Amiloride selectively blocks the low threshold (T) calcium channel. *Science* **240**, 213–215.

THOMAS, E. & PIERCE, A. G. E. (1964). The solitary active cells: histochemical demonstration of damage-resistant nerve cells with the a TPN-diaphorase reaction. *Acta Neuropathologica* **3**, 238–249.

TOTH, P. T., BINDOKAS, V. P., BLEAKMAN, D., COLMERS, W. F. & MILLER, R. J. (1993). Mechanism of presynaptic inhibition by neuropeptide Y at sympathetic nerve terminals. *Nature* **364**, 635–639.

VIZZARD, M. A., ERDMAN, S. L., FÖRSTERMANN, U. & DE GROAT, W. C. (1994). Differential distribution of nitric oxide synthase in neural pathways to the urogenital organs (urethra, penis, urinary bladder) of the rat. *Brain Research* **646**, 279–291.

XU, Z.-J. & ADAMS, D. J. (1992). Voltage-dependent sodium and calcium currents in cultured parasympathetic neurones from rat intracardiac ganglia. *Journal of Physiology* **456**, 425–441.

XU, Z.-J. & ADAMS, D. J. (1993). α-Adrenergic modulation of ionic currents in cultured parasympathetic neurons from rat intracardiac ganglia. *Journal of Neurophysiology* **69**, 1060–1070.

ZHU, Y. & IKEDA, S. R. (1993). Adenosine modulates voltage-gated Ca^{2+} channels in adult rat sympathetic neurons. *Journal of Neurophysiology* **70**, 610–620.

Acknowledgements

Correspondence and reprint requests should be addressed to S. R. Ikeda. We are grateful to Dr Thomas M. Mills for showing us the anatomy of the rat MPG and arousing our interest in this topic, and Dr William G. Dail for discussion. The research was supported in part by grants from the National Institutes of Health and the Georgia Affiliate of the American Heart Association (to S.R.I.).

Author's present address

Y. Zhu: Laboratory of Cellular and Molecular Pharmacology, National Institute of Environmental Health Sciences, Research Triangle Park, NC 27709, USA.

Received 31 January 1995; accepted 26 May 1995.